

A novel hybrid numerical with analytical approach for parameter extraction of photovoltaic modules

Dris Ben hmamou^{a,*}, Mustapha Elyaqouti^b, El hanafi Arjidal^a, Driss Saadaoui^b,
Souad Lidaighbi^b, Jamal Chaoufi^a, Ahmed Ibrahim^{c,d}, Rabya Aqel^a, Daoudi El fatmi^a,
Sergey Obukhov^c

^a Laboratory of Electronics, Signal Processing and Physical Modeling, Faculty of Sciences of Agadir Ibn Zohr University, BP 8106, 80000 Agadir, Morocco

^b Materials and Renewable Energy Laboratory, Agadir Faculty of Sciences, Ibn Zohr University, BP 8106, 80000 Agadir, Morocco

^c National Research Tomsk Polytechnic University, Tomsk 634050, Russia

^d Electrical Power & Machines Department, Faculty of Engineering, Zagazig University, Egypt

ARTICLE INFO

Keyword:

Photovoltaic
Single diode model
Mono-crystalline
Thin film
Shell SP140
Iterative approach

ABSTRACT

Building an accurate mathematical model of photovoltaic modules is an essential issue for providing reasonable analysis, control and optimization of photovoltaic energy systems. Therefore, this study provides a new accurate model of photovoltaic Panels based on single diode Model. In this case, the proposed model is the link between two models which are the ideal model and the resistance network. All parameters are estimated based on hybrid Analytical/Numerical approach: three parameters photocurrent, reverse saturation current and ideality factor are obtained using an Analytical approach based on the datasheet provided by the manufacturer under Standard Test Conditions. The series and shunt resistances are obtained by using a Numerical approach similar to the Villalva's method in order to achieve the purpose of modeling the resistance network part. Our model is tested with data from the manufacturer of three different technologies namely polycrystalline, Mono-crystalline silicon modules and thin-film based on Copper Indium Diselenide, and for more accurate performance evaluation we are introducing the Average Relative Error and the Root Mean Square Error. The simulated Current-Voltage and Power-Voltage curves are in accordance with experimental characteristics, and there is a strong agreement between the proposed model and the experimental characteristics. The computation time is 0.23 s lower than those obtained using others approach, and all obtained results under real environment conditions are also compared with different models and indicated that the proposed model outperforms the others approach such as villalva's and kashif's method.

Introduction

As a result of the pollution of fossil fuels and its rising prices, deterioration of the environmental quality and air pollution with the greenhouse gases such as CO₂ and CH₄, some activities are raised worldwide in terms of technology to access clean and renewable energy [1]. Thanks to renewable energies benefits from the dynamic of the Kyoto Protocol, which favors this solution in the fight against greenhouse gases [2,3], the Photovoltaic power market has grown rapidly in the last decade, and the share of renewable energies in the world's electricity mix had an exponential growth over the last years [4]. Along with several technologies, namely wind and solar, have reached a real

technical maturity and are now competitive compared to a cost of energy integrating the value of CO₂ [5,6]. Among all renewable energy sources, solar energy is the most promising energy [7]. Photovoltaic systems represent the most direct way to convert solar energy into electrical energy by utilizing the inherent properties of semiconductors [8]. The cost of PV systems is always higher, so prior to installation a modeling and characterization study of PV modules is required before installation [1]. So it is always desirable to have a model which allows studying the behavior of solar cells [7], i.e. Use the equivalent electrical circuit built with diodes and resistors to build a model suitable for the experimental data [9]. Over the years, many models have been proposed, starting from single diode model, to the R_s-model, the R_p-model as well as two and three diode models [10,11]. The most widely

* Corresponding author at: Laboratory of Electronics, Signal Processing and Physical Modeling, Faculty of Sciences of Agadir Ibn Zohr University, BP 8106, 80000 Agadir, Morocco.

E-mail address: benhmamou.dris@edu.uiz.ac.ma (D. Ben hmamou).

<https://doi.org/10.1016/j.ecmx.2022.100219>

Received 4 January 2022; Received in revised form 8 March 2022; Accepted 28 March 2022

Available online 30 March 2022

2590-1745/© 2022 The Authors. Published by Elsevier Ltd. This is an open access article under the CC BY-NC-ND license (<http://creativecommons.org/licenses/by-nc-nd/4.0/>).

Nomenclature			
ARE	Average Relative Error	V_{ocn}	Open circuit voltage of the PV panel at STCs (V)
K	Boltzmann constant ($1.381.10^{-23}$ J/K)	β_v	Open circuit voltage temperature coefficient ($V/^\circ C$)
I-V	Current-Voltage characteristic	I_{pv}	Photocurrent (A)
CIS	Copper Indium Diselenide	I_{pvn}	Photocurrent at STCs (A)
A	Diode ideality factor	T	PV cell temperature ($^\circ C$)
q	Electric charge of an electron ($1.602.10^{-19}C$)	T_n	PV cell temperature at STCs ($^\circ C$)
P_{max_esti}	Estimated power at the maximum power point (W)	I_{sn}	Reverse saturation current of the diode at STCs (A)
P_{max_exp}	Experimental power at the maximum power point (W)	I_s	Reverse saturation current of the diode (A)
E_g	Gap energy of solar cell(eV)	RMSE	Root Mean square Error (A)
IAE	Individual Absolute Error	β_i	Short circuit current temperature coefficient ($A/^\circ C$)
MPP	Maximum power point	R_p	Shunt resistance (Ω)
N_s	Number of cells connected in series	STCs	Standard Test Conditions
I_{mp}	Output Current at MPP(A)	R_s	Series resistance (Ω)
V_{mp}	Output Voltage at MPP(V)	I_{sc}	Short circuit current of the PV module (A)
V_{oc}	Open circuit voltage of the PV panel (V)	I_{scn}	Short circuit current of the PV module at STCs (A)
		G	Solar irradiance (W/m^2)
		G_n	Solar irradiance at STCs ($1000 W/m^2$)

modeling methods that have high accuracy based on Artificial Intelligence like the Meta-Heuristic approach and Evolutionary algorithms summarized in Table.1 require solving implicit equations of output voltage and current, hence increasing the complexity of the approach. Obviously, the more complicated a model is, the more parameters are involved in its computation [9]. There are also, Analytical and Numerical methods such as these summarized in Table.2. In this paper we are adopted the single diode model and focus our attention on the extraction of all model parameters at STCs ($T = 298$ K, $G = 1000$ W/m^2) namely photo generation current I_{pv} , leakage current I_s , Ideality factor of the diode A, series resistance R_s and shunt resistance R_p . And study the impact of input solar radiation G and temperature T on our model parameters. Table 3 shows a literature reviews of these parameters with increasing temperature and irradiation.

The Novelty of this study is provide an improved hybrid analytical/Numerical approach that has no implicit equation to deal with, in order to explore and discuss the behavior of the single diode parameters under real environmental conditions in order to characterizing PV modules. The performance of this method is evaluated using the datasheet provided by the manufacturers of the three PV modules such as Monocrystalline Shell SP140 [59], Poly-crystalline Shell S75[60] and thin film Shell ST20 for different temperatures in the range of $20^\circ C - 60^\circ C$ and different irradiation and in the range of $200W/m^2 - 1000W/m^2$ for three photovoltaic modules. All associated calculation methods that we have evaluated are done by using Matlab Script.

The remainder of this paper is organized in the following manner. After an introduction, Section 2 describes the modelling of the photovoltaic modules used in this study organized in two step, the first is for extract I_{pv} , I_s and A. In the second one the series and shunt resistances R_s and R_p , are calculated by using an iterative approach. Finally, we preset in section 3, all obtained result compared with some well-known modeling methods.

Modeling the PV module

The performance of the Photovoltaic cell is mainly based on the selection of Photovoltaic model and associated parameters, in practice two predominant types, these are single diode Photovoltaic model [61] and double diode Photovoltaic models [62]. But the authors[62,63] have evaluated that the double diode PV model is expensive than to the single diode model.

The Single-Diode model

The equivalent circuit of the single-diode model of photovoltaic module is shown in Fig. 1.

Applying Kirchhoff's current and voltage laws, the Output Current and Output Voltage relation of the photovoltaic devise can be obtained as:

$$I = I_{pv} - I_s \times \left\{ \exp \left[\frac{V + R_s \times I}{A \times V_t} \right] - 1 \right\} - \frac{V + R_s \times I}{R_p} \quad (1)$$

where:

I_{pv} is the photocurrent generated bay photovoltaic module under illumination, I_s is the reverse saturation current of the diode, A is the diode ideality factor, R_s is the series resistance used to characterize the resistance of electrode surface, R_p is the shunt resistance used to characterize the leakage current of P-N junction. V_t is the thermal voltage given bay expression: $V_t = \frac{K \times T \times N_s}{q}$ where K is the Boltzmann constant ($1.38.10^{-23}J/K$), q is the electron charge ($1.67.10^{-19}C$), N_s and T are the number of cells in series and the cell temperature, respectively. While in order to design a single-diode photovoltaic model, five electrical parameters must be evaluated.

The current Voltage characteristic that represents Eq. (1) is shown in Fig. 2. Three remarkable points are highlighted such as the open circuit voltage V_{oc} , the short circuit current I_{sc} and the maximum power point (MPP).

As it was adopted in [64] the equivalent circuit model of photovoltaic module used in this study shown in Fig. 1 is divided into the ideal model part and the resistance network part. The Current-Voltage characteristic expression of the ideal model part is given as follow:

$$I_{id} = I_{pv} - I_s \times \left\{ \exp \left[\frac{V_{id}}{A \times V_t} \right] - 1 \right\} \quad (2)$$

where I_{id} and V_{id} are the output current and output voltage of the ideal model part, respectively. So it is a simple equation to solve without the need for a numerical approach.

Parameter extraction

In this study the proposed model will be split into two parts. The first part is purely analytical regards the estimation of three parameters I_{pv} , I_s and A. The value of R_p and R_s is extracted in step 2 using an Iterative

Table 1

The literature reviews of Analytical/Numerical approach used for PV parameter estimation.

Ref	Approach	Results and some data paper
Sheraz and Abido 2014[12]	Hybrid approach Differential Evolution/ Fuzzy Logic	The authors provide an efficient differential evolution (DE) that requires only the available data to estimate the five parameters of the electric circuit model of PV systems. Sunpower Photovoltaic module is used to validate the proposed model. Also, fuzzy logic based (FLC) MPPT controller is also adopted and compared with the conventional incremental conductance method. From all obtained results showed that the FLC MPPT has fast convergence speed, less fluctuation in the steady state and may not fail under quickly varying operating conditions.
Zagrouba et al. 2010 [13]	Genetic Algorithms (GAs)	Zagrouba et al introduce a numerical technique based on GAs formulated as a non-convex optimization problem and using algorithm of Newton Raphson to identify the electrical parameters of photovoltaic solar cells and modules. The study conducts to less satisfactory results which depend on the initial conditions leading to local minima solutions. The GAs overcomes problems involved in the local minima.
Saadaoui et al. 2021 [14]	Genetic Algorithm based on Non-Uniform Mutation (GAMNU)	Saadaoui et al introduce this new improved genetic algorithm based on search operators “the mutation non-uniform and Blend crossover (BLX- α)”. The authors use for validate their approach R.T. C. France, Photowatt-PWP 201, STP6-120/36 and ESP-160 PPW PV cells. The performance results of the proposed GAMNU algorithm show a very high similarity between the estimated curves and the experimental data.
Ben Hmamou et al. 2021[7]	Particle Swarm Optimization (PSO)	The PSO approach is based on the behavior of social organisms such as bird flocking and fish schooling. The performance is tested by using the photovoltaic cell R. T.C France, based on the experimental values. The values of RMSE obtained are very low and less than those obtained by others soft computing algorithm
Ketkar and M. Chopde 2014[15]	Artificial Bee Colony (ABC)	Ketkar et al added some modifications implemented in traditional ABC algorithm. All of them demonstrate ability of modified algorithm to be primary candidate for the parameter extraction in wide search space.
	Bacterial Foraging Optimization (BFO)	BFO algorithm minimized using global heuristic

Table 1 (continued)

Ref	Approach	Results and some data paper
Awadallah, Venkatesh and Member, 2016[16]		optimization algorithms an objective function based on difference between computed and targeted performance given in the manufacturer datasheet at STCs. This study reveals that the reproduction event contributes to the rapid convergence of the bacterial population to the optima. Also, The obtained results indicated that exist a good matching between experimental measurements and estimated performance, and shows the accuracy of modeling.
Jacob et al., 2015[17]	Artificial Immune System (AIS)	Jacob et al introduce AIS method that used A new objective function based on derivative of maximum power with respect to voltage. The result indicated that AIS approach outperforms the GA and PSO algorithms. Also, AIS approach can be used for parameter extraction of panel with different make and models.
Mirbagheri, Mirbagheri and Mokhlis, 2014[18]	Imperialist Competitive Algorithm (ICA)	ICA approach allowed the authors to find the optimal number of components of the proposed Hybrid Renewable Energy System with the lowest possible cost
Kharchouf et al [19]	Differential Evolution (DE)	In this study DE algorithm was used to estimate the electrical circuit parameters of a SDM and DDM. The Lambert W function allowed the reconstruction of the I-V and P-V characteristic. R.T.C. France solar cell, Schutten solar STM6-40/36 and the Photowatt-PWP 201 modules are used for validate DE model. All obtained results are compared with GA, PSO in terms of accuracy, consistency, speed of convergence, computation time, and gives reliable results for all SDM parameters with low RMSE values between simulated and experimental I-V and P-V curves.
Dali, Bouharchouche and Diaf, 2015[20]	GA-PSO	The hybrid method has demonstrated a very high ability to modeling, and extracts all parameter of SDM and DDM with a very low RMSE and to identify the model parameters with good accuracy.
Majid Dehghani et al [21]	Fuzzy Logic Controller (FLC)	Majid Dehghani et al proposed a new FLC for Maximum Power Point Tracking. In this study all parameters of FLC have been estimated by using hybrid approach PSO-GA. The performance of the proposed PSO-GA based on optimized FLC has been investigated

(continued on next page)

Table 1 (continued)

Ref	Approach	Results and some data paper
		with rapid changes of temperature and irradiation. The obtained result indicate that the Proposed model outperforms the P&O, INC, GA based FLC and PSO based optimizer FLC.
Bahrani Prakash and Naveen Jain[22]	P&O and FLC	Bahrani Prakash and Naveen Jain introduce in this study two different MPPT methods, P&O and (FLC). The performance of both proposed method has been tested under STCs and dynamic tests conditions. The simulation results show that the FLC provides improved results for output power compared with the P&O method.
Madeti and Singh, 2018[23]	k-Nearest Neighbors (kNN)	Madeti and Singh uses for the first time the kNN rule based method to detect and classify the fault as well as locate the faulted string of the PV array in a typical grid tied distributed inverter PV system The obtained simulation results provide excellent classification accuracy for the defects tested.
Zhu et al., 2018[24]	Gaussian kernel-Fuzzy C Means (GK-FCM)	FCM algorithm based on artificial intelligence and fuzzy information processing function to perform unsupervised clustering of defect samples and solves the problem of classification of the sample data of JKM245p modules.
Douiri, 2019[25]	Neuro-Fuzzy system tuned by Particle Swarm Optimization algorithm (PSO-NF)	The hybrid PSO-NF approach was applied to simulate the experimental power-voltage and current-voltage characteristics of SPM085P-BP PV module. The resulting models fit well in both cases, and the learning speed is fast.
Böök et al., 2020[26]	Quality control approach (QC)	The QC method gives a good filtration of non-realistic calculated normal direct radiation data, and provides a potential technique to be implemented
Li et al., 2021[27]	Artificial Neural Network (ANN)	The Multi-Neural Network (MANN) Method is applied to experimental data of Monocrystalline (x-Si), Polycrystalline (m-Si), (CdTe) and (CIGS) PV modules. The performance is compared with a single-ANN. The results indicate that the proposed MANN method has a more accurate output performance prediction.

approach. The algorithm has been tested using Matlab software.

Step 1: Analytical approach

Based on Eq.(1) and at the short circuit point ($I = I_{sc}; V = 0$), the short circuit current I_{sc} is given as follow:

$$I_{sc} = I_{pv} - I_S \times \left\{ \exp \left[\frac{R_S \times I_{sc}}{A \times V_t} \right] - 1 \right\} - \frac{R_S \times I_{sc}}{R_p} \quad (3)$$

As it can be assumed that $\exp \left[\frac{R_S \times I_{sc}}{A \times V_t} \right] \approx 1$ because R_S can be neglected.

After simplification we obtain finally the expression of photocurrent generated bay photovoltaic cells at STCs given bay:

$$I_{pvn} = I_{scn} \left(1 + \frac{R_S}{R_p} \right) \quad (4)$$

Under real condition the current generated by the incident light is directly proportional to the Sun irradiation and with the Temperature, then is linear increase with increasing the Temperature and the Sun irradiation according to the following equation [65,66]:

$$I_{pv} = (I_{pvn} + \beta_I(T - T_n)) \times \frac{G}{G_n} \quad (5)$$

Herein G , G_n , β_I , T , T_n and I_{pvn} are instantaneous solar irradiances and Standard Test Conditions (STCs) irradiance, is the temperature coefficient of current, the cell junction ambient and nominal Temperatures, the light generated current at STCs, respectively.

And at the open circuit point ($I = 0; V = V_{oc}$) Eq.(1) becomes:

$$0 = I_{pv} - I_S \times \left\{ \exp \left[\frac{V_{oc}}{A \times V_t} \right] - 1 \right\} - \frac{V_{oc}}{R_p} \quad (6)$$

We obtain the following expression:

$$I_{pv} = I_S \times \left\{ \exp \left[\frac{V_{oc}}{A \times V_t} \right] - 1 \right\} + \frac{V_{oc}}{R_p} \quad (7)$$

After, the saturation current I_S can be simplified as Eq.(8):

$$I_S = \frac{I_{sc} \left(1 + \frac{R_S}{R_p} \right) - \frac{V_{oc}}{R_p}}{\exp \left[\frac{V_{oc}}{A \times V_t} \right] - 1} \quad (8)$$

And as R_p is very large and R_S can be neglected, then we can assume that: $\frac{V_{oc}}{R_p} \approx 0$

And from Eq.(4) and Eq.(8) the expression of I_S becomes:

$$I_S = \frac{I_{pv}}{\exp \left[\frac{V_{oc}}{A \times V_t} \right] - 1} \quad (9)$$

And at real condition and as I_S slightly dependent on irradiation, Eq. (9) can be simplified as:

$$I_S = \frac{(I_{pvn} + \beta_I(T - T_n))}{\exp \left[\frac{V_{ocn} + \beta_I(T - T_n)}{A \times V_t} \right] - 1} \quad (10)$$

Also Several researchers [67,65,66,68,69] have evaluated that these parameter is proportional to the cube of the photovoltaic cells temperature, as shown in Eq.(11) :

$$I_S = I_{sn} \times \left(\frac{T_n}{T} \right)^3 \times \exp \left[\frac{q \times E_g}{A \times K} \left(\frac{1}{T_n} - \frac{1}{T} \right) \right] \quad (11)$$

where:

$$I_{sn} = \frac{I_{scn}}{\exp \left(\frac{V_{ocn}}{A \times V_t} \right) - 1} \quad (12)$$

Herein I_{sn} , E_g are the nominal saturation current, the band gap energy of the semiconductor ($E_g = 1.12$ for the polycrystalline Si at 25 °C [65,61]), respectively. The values of I_S versus the temperature found by Eqs.(10), (11) are grouped together in the Table 4.

Fig. 3 represents the variation of I_S as a function of the temperature.

Table 2
The literature reviews of Meta-heuristic algorithms used for PV parameter optimization.

Ref	approach	Model type	Type of solar cell	Result
Lidaighbi et al. 2021[28]	Hybrid Approach Numeric/Analytical	SDM	Shell SP70 Shell SP70	the analytical techniques estimate the current–voltage curve and the power-voltage curve at STCs with excellent accuracy and almost the same performance as the numerical method
Louzazni et al. 2019[29]	Lagrange Multiplier Method (LMM)	SDM	R.T.C France Photowatt-PWP 201.	Used to find the power and current–voltage characteristics as objective and constraint functions. It’s easy to used based on characteristics functions of solar cell
Qais, Hasanien, and Alghuwainem 2019[30]	Hybrid Analytica/ sunflower optimization (SFO) algorithm	TDM	KC200GT MSX-60CS6K-280 M	applied to extract seven optimal parameters ($n_3, I_{01}, I_{02}, I_{03}, n_1, n_2$ and R_s) and other parameters (R_p and I_{ph}) are calculated analytically.
Toledo and Blanes 2016 [31]	Analytical and Quasi-Explicit (AQE)	SDM	R.T.C France	AQE method, able to obtain the five parameters of the solar cell single-diode model just using four arbitrary points of the I-V curve and their slopes
Ruschel et al. 2016[32]	unnamed	SDM	Multi-crystalline, Mono-crystalline, CIGS, Tandem, Amorphous and CdTe	Difficulty to apply the model on all PV module because a large variation was found during the simulation of Rp.
Tong and Pora 2016[33]	Approach based on intrinsic property of solar cells	SDM	Polycrystalline mono-crystalline, thin film panels. For example: -Model STM6-40/36 -STP6-120/36	This model is not valid for polycrystalline module technology but gives good results for other technologies.
Bogning Dongue, Njomo, and Ebengai 2013[34]	a nonlinear analytical five-point model	SDM / DDM	Monocrystalline: SM55 Multi-Crystalline: S75 Thin-film: ST40	The model is valid in all points of I-V and P-V characteristics, based only on the manufacturer’s data.
Deihimi, Naghizadeh, and Meyabadi 2016[35]	Unnamed	SDM	R.T.C. France	The main aim of the proposed method is providing an accurate tool for derivation of model parameters. This method is providing high selective capability for users of PV module according to their systems.
A. Laudani et al. 2015[36]	Unnamed	SDM	CEC6PPVMSanyo HIT-N225A01	With a low iteration number, the model is able to extract the parameters with a high degree of accuracy.
Batzelis et al. 2015 [37]	Unnamed	SDM	Conergy Power Plus 190PC, Day4 Energy 60MC-I, Perlight PLM-250P-60, Solea SM 190 Yingli YL-165	New coefficient was introduced, This coefficient was used to derive an analytical expression for the diode ideality factor of the model using only datasheet information.
Silva et al. 2016[38]	Unnamed	SDM	Polycrystalline PV Panel Kyocera KC200GT, Polycrystalline PV Panel Kyocera KS20T	In this study A new error metric MAEP was defined and two different methods based on two different error metrics, MAEP and NRMSD are proposed.
Antonino Laudani, Riganti Fulginei, and Salvini 2014[39]	Unnamed	SDM	Mono-crystalline, Multi-crystalline silicon Suntech STP-280 SunPower SPR-315 Atersa A-120 Atersa A-130 Isotofon I-110	a fully mathematical approach was used to gain insight to the five-parameter model related to the one-diode equivalent circuit
Zaimi et al. 2019 [40]	Unnamed	SDM	KC130GT SM55 PV	Three parameters are expressed in terms of Ideality factor and photovoltaic metrics. The optimized values of model-physical parameters are obtained by minimizing RMSE of the output current.
Tutkun, Elibol, and Aktas 2015[41]	shuffled frog leaping algorithm (SFLA)	SDM	Monocrystalline and Polycrystalline	The SFLA approach has produced significant and encouraging results in the vicinity of MPP.

Table 3
The literature reviews of single diode parameters with increasing temperature and irradiance.

Parameter	Increasing Temperature	Increasing Irradiance
I_{pv}	Linear increase [42]	Linear increase [42]
I_s	Polynomial increase [43] Exponential increase [44,45] Decrease [46] increase[47]	Exponential increase[48] Decrease [46] increase[49]
A	Linear decrease [50,51] Invariant[47,52]	Linear increase[48] Linear decrease[50]
R_s	Linear increase[43] Linear decrease[50,52] Exponential decrease[44] Exponential increase[53] Increase[54]	Invariant[48] Decrease[46,49] Increase [55,56]
R_p	Linear decrease[43,50,52] Decrease [47]	Linear decrease[48,50] Decrease[49,56,57] Inverse decrease[32] Invariant[58]

From this figure we can see that the two expressions of I_s Eq.(10) and Eq. (11) give the same values at low temperature and at high temperature there is a small difference which can be neglected.

The ideality factor A is thus an important input parameter in the description of the solar cell’s electrical behaviour. Their value is may be arbitrarily chosen [70], and many authors discuss ways to estimate the correct value of this parameter[71 72], usually $A \leq 1.5$. In this study we can obtained the value of A using two method. The first, when we take into account the previous assumption in Eq. (7) we can express V_{oc} by:

$$V_{oc} = A \times V_t \times \log \left[\frac{I_{pv}}{I_s} + 1 \right] \tag{13}$$

Take into account Eq. (5) and equation Eq. (10) we can obtain:

$$V_{oc} = A \times V_t \times \log \left[\frac{(I_{pvn} + \beta_I(T - T_n)) \times \frac{G}{G_n} + 1}{\frac{(I_{pvn} + \beta_I(T - T_n))}{\exp \left[\frac{V_{ocn} + \beta_V(T - T_n)}{A \times V_t} \right] - 1}} + 1 \right] \tag{14}$$

Finally, the expression of the diode ideality factor can be expressed

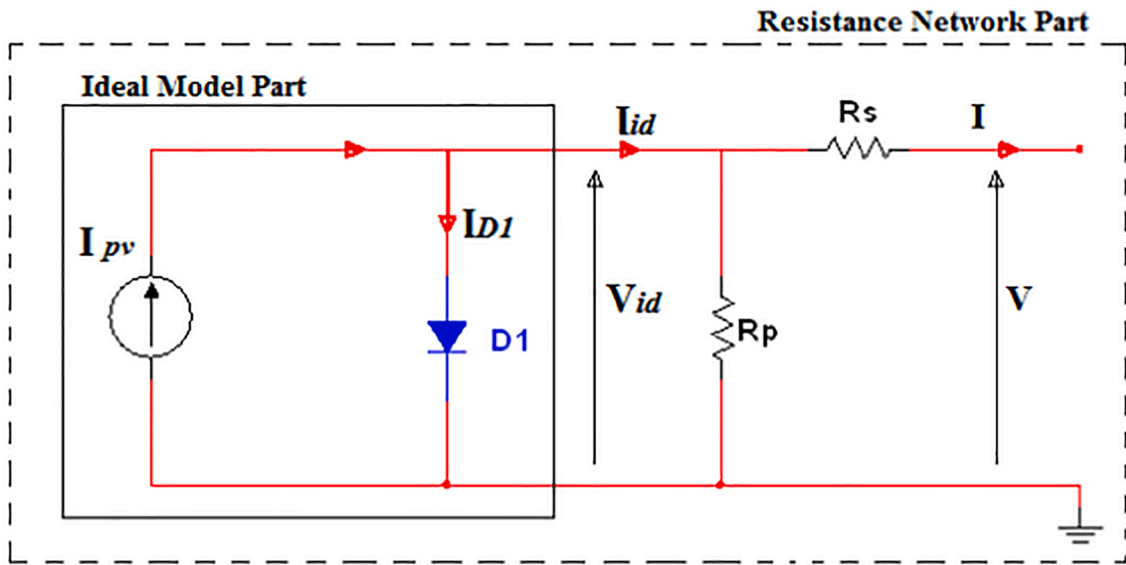


Fig. 1. Equivalent Circuit Model of photovoltaic module.

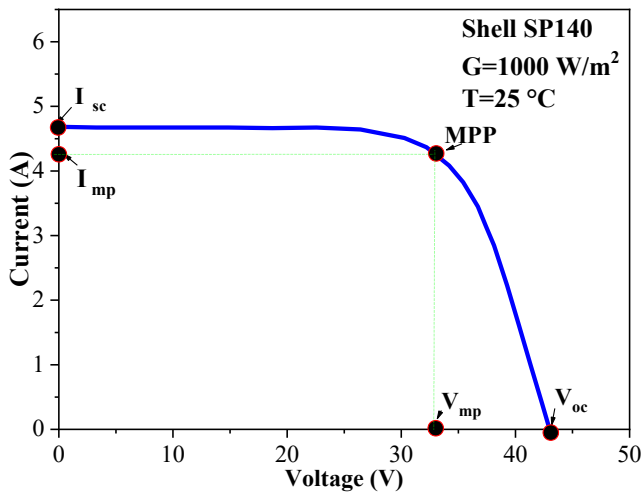


Fig. 2. The I-V curve adjusted to three remarkable points for Shell SP140 module.

Table 4

The estimated value of the reverse saturation current of the diode of Shell SP140 Module using Eq. (10) and Eq. (11).

Temperature (°C)	reverse saturation current Is (mA) Eq.(10)	reverse saturation current Is (mA) Eq.(11)
20	$5,41788.10^{-7}$	$5,39775.10^{-7}$
30	$1,58027.10^{-6}$	$1,58555.10^{-6}$
40	$4,30566.10^{-6}$	$4,36135.10^{-6}$
50	$1,10280.10^{-5}$	$1,13016.10^{-5}$
60	$2,77355.10^{-5}$	$2,77355.10^{-5}$

as:

$$A = \frac{V_{oc} - (V_{ocn} + \beta_v(T - T_n))}{V_t \times \log\left(\frac{G}{G_n}\right)} \quad (15)$$

where we can calculate the value of A the diode factor ideality using the Nominal Operating Cell Temperature Conditions (NOCT):

$$T = T_{NOCT}$$

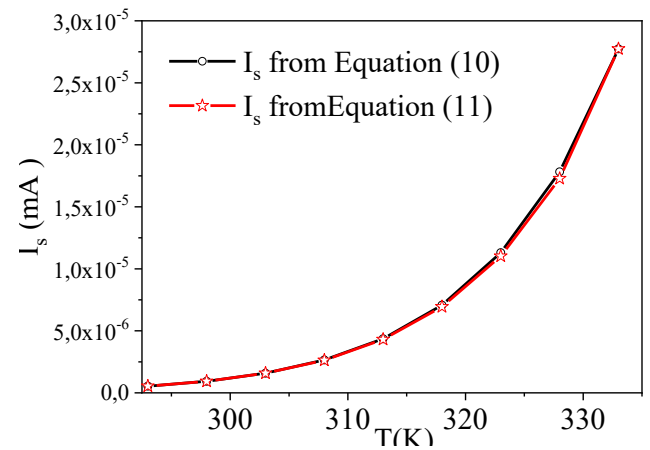


Fig. 3. The Is versus T curve of Shell SP140 Module using Eq.10 and Eq.11.

$$A = \frac{V_{oc_NOCT} - (V_{ocn} + \beta_v(T_{NOCT} - T_n))}{V_t_NOCT \times \log\left(\frac{G_{=NOCT}}{G_n}\right)} \quad (16)$$

where

V_t_NOCT represent the thermal voltage at $T = T_{NOCT}$ that given with expression below:

$$V_t_NOCT = \frac{K \times T_NOCT}{q} \quad (17)$$

The second method focused on the ideal part of the equivalent circuit shown in Fig. 1, the output current represents in Eq. (2) become at maximum power point current as: ($V_{id} = V_{mp}$; $I_{id} = I_{mp}$).

$$I_{mp} = I_{pv} - I_s \times \left\{ \exp\left[\frac{V_{mp}}{A \times V_t}\right] - 1 \right\} \quad (18)$$

$$I_s \times \left\{ \exp\left[\frac{V_{mp}}{A \times V_t}\right] - 1 \right\} = I_{pv} - I_{mp} \quad (19)$$

At $T = T_n$ Eq. (12) becomes:

$$I_S = \frac{I_{pvn}}{\exp\left[\frac{V_{ocn}}{A \times V_{tn}}\right] - 1} \quad (20)$$

At short circuit current $I_{pvn} = I_{scn}$ (ideal part), Eq. (19) becomes:

$$\frac{I_{pvn}}{\exp\left[\frac{V_{ocn}}{A \times V_{tn}}\right] - 1} \times \left\{ \exp\left[\frac{V_{mp}}{A \times V_{tn}}\right] - 1 \right\} = I_{pvn} - I_{mp} \quad (21)$$

$$\frac{1}{\exp\left[\frac{V_{ocn}}{A \times V_{tn}}\right] - 1} \times \left\{ \exp\left[\frac{V_{mp}}{A \times V_{tn}}\right] - 1 \right\} = 1 - \frac{I_{mp}}{I_{scn}} \quad (22)$$

We take account the assumption: $\exp\left[\frac{V_{ocn}}{A \times V_{tn}}\right] \gg 1$ and $\exp\left[\frac{V_{mp}}{A \times V_{tn}}\right] \gg 1$

$$\frac{\exp\left[\frac{V_{mp}}{A \times V_{tn}}\right]}{\exp\left[\frac{V_{ocn}}{A \times V_{tn}}\right]} = \left(1 - \frac{I_{mp}}{I_{scn}}\right) \quad (23)$$

$$\frac{V_{mp} - V_{ocn}}{A \times V_{tn}} = \ln\left(1 - \frac{I_{mp}}{I_{scn}}\right) \quad (24)$$

Finally, the expression of the diode ideality factor for ideal part as:

$$A = \frac{V_{mp} - V_{ocn}}{V_{tn} \times \ln\left(1 - \frac{I_{mp}}{I_{scn}}\right)} \quad (25)$$

Finally, we are obtained two expressions of the diode ideality factor: Eq. (25) and Eq. (16). The first expression depends with ideal part and the last one depends with network resistance part of the equivalent circuit. The values obtained using these expressions are summarized in Table 5.

We can see that the expression found by the ideal part of the circuit is far from reality. In the end the expression that we will adopted to find the values of ideality factor A is Eq. (25).that of the resistance network part

Step 2: Iterative solution of R_s and R_p

The value of two parameters shunt and series resistances R_p , R_s , respectively are obtained through iteration approach. Several researchers have evaluated these two parameters graphically using the datasheet provided by the manufacturers [64], but in this study, the series and shunt resistances are calculated simultaneously, similar to the procedure proposed in [67].

The initial value of R_p is the slope of the line segment between short-circuit and the maximum power points, their expressions is shown in Eq. (26),

$$R_p = \frac{V_{mp}}{I_{scn} - I_{mp}} - \frac{V_{ocn} - V_{mp}}{I_{mp}} \quad (26)$$

and for series resistance R_s the initial condition is $R_s = 0$.

At the best operating point ($V = V_{mp}; I = I_{mp}$) of the system, the corresponding output current is given bay:

$$I_{mp} = I_{pv} - I_S \times \left\{ \exp\left[\frac{V_{mp} + R_s \times I_{mp}}{A \times V_{tn}}\right] - 1 \right\} - \frac{V_{mp} + R_s \times I_{mp}}{R_p} \quad (27)$$

Table 5
The estimated values of the diode ideality factor for Shell SP140 Module.

Photovoltaic modules	from Eq.16(ideal part)	from Eq.25(resistance part)
Shell SP140	2.26	1.2714
Shell S75	1.90	1.40
Shell ST20	3.80	1.35

$$\frac{V_{mp} + R_s \times I_{mp}}{R_p} = I_{pv} - I_S \times \left\{ \exp\left[\frac{V_{mp} + R_s \times I_{mp}}{A \times V_{tn}}\right] - 1 \right\} - I_{mp} \quad (28)$$

$$\frac{R_p}{V_{mp} + R_s \times I_{mp}} = \frac{1}{I_{pv} - I_S \times \left\{ \exp\left[\frac{V_{mp} + R_s \times I_{mp}}{A \times V_{tn}}\right] - 1 \right\} - I_{mp}} \quad (29)$$

Finally the expression for R_p can be rearranged and rewritten as:

$$R_p = \frac{V_{mp} + R_s \times I_{mp}}{I_{pv} + I_S \times \left\{ \exp\left[\frac{V_{mp} + R_s \times I_{mp}}{A \times V_{tn}}\right] - 1 \right\} - I_{mp}} \quad (30)$$

From Fig. 1 and by using the resistance network part the Output Current and Voltage of the photovoltaic module can be determined using the Eq. (31) and Eq. (32), respectively.

$$I = I_{id} - \frac{V_{id}}{R_p} \quad (31)$$

$$V = V_{id} - R_s \times I \quad (32)$$

where equation Eq.(5) and Eq.(6) are solved to obtain the estimated Current-Voltage characteristic curve of the proposed model of photovoltaic module [64].

Then we can calculate the estimated power of the photovoltaic module using the expressions as shown in Eq. (33).

$$P_{estimated} = I \times V \quad (33)$$

R_s is iteratively incremented and at each iteration the value of the shunt resistance R_p is calculated using Eq.(30), then the value of output current and voltage are updated using Eq.(31) and Eq.(32), until the experimental power provided by the manufacturers is confused (or near) with the value of the estimated power calculated by Eq. (33). When this condition is reached we keep the values of R_s and R_p correspond to this iteration. Fig. 4 shows the flowchart of extraction of all parameters for the proposed model.

Results and discussion

The Electrical characteristics at STCs and NOCT conditions and the temperature coefficients for open circuit voltage and short circuit current of the used photovoltaic modules are summarized in Table 6.

Verification of the open circuit voltage

From Eq. (14) we can see that the open circuit voltage V_{oc} depends of the temperature T and irradiation G . The estimated and experimental values of V_{oc} for Shell SP140 module at several values of temperature and Irradiation and the corresponding Individual Absolute Error (IAE) of the V_{oc} calculated by using Eq.(34) are tabulated in Table 7. It can be seen that the calculated values under different temperature and irradiation are very close to the experimental values.

$$IAE_{Voc} = \left| (V_{oc})_{estimated} - (V_{oc})_{experimental} \right| \quad (34)$$

The estimated values of V_{oc} compared with their provided by the manufacturers are represented in Fig. 5 when T changes and $G = 1000W/m^2$, and in Fig. 6 when G change and $T = 25^\circ C$.

From Fig. 5 and Fig. 6 we can conclude that the maximum value of IAE_{Voc} is equal to 0.17 V when $G = 600W/m^2$ and equal to 0.2V when $T = 60^\circ C$, indicate that the obtained results has significantly better accuracy of V_{oc} between the data provided by the manufacturer and the estimated value using Eq.(14) of proposed model.

Verification of Current-Voltage characteristic curves

In this study the five parameters of proposed model are calculated

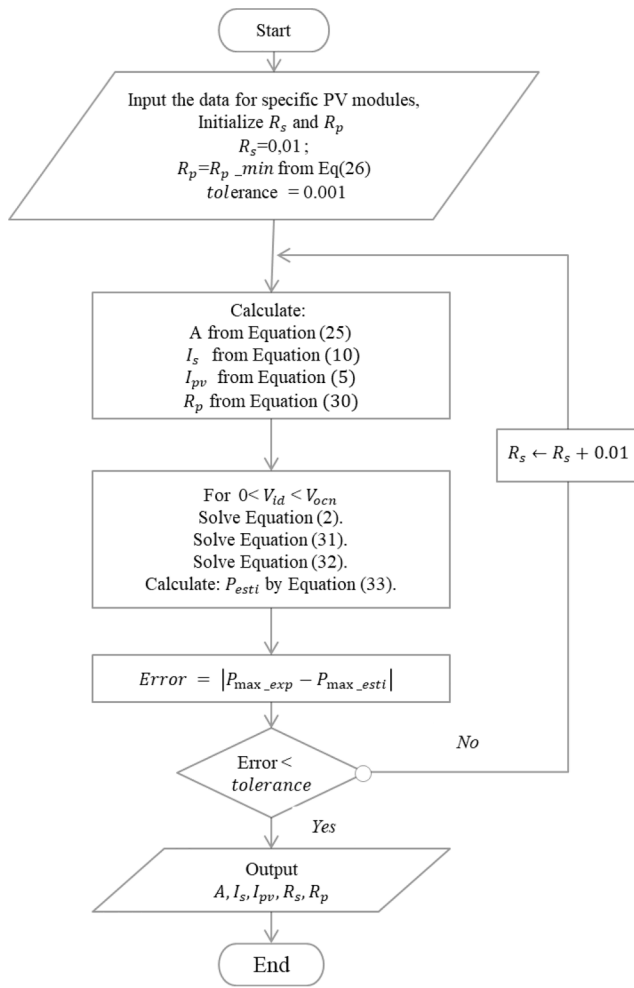


Fig. 4. Flowchart of extraction of all parameters model.

Table 6

Electrical characteristics of the used photovoltaic module:

Photovoltaic module	PolycrystallineShell SP140	MonocrystallineShell S75	Thin film Shell ST20
I_{scn} (A)	4.7	4.7	1.54
V_{ocn} (V)	42.8	21.6	22.9
I_{mp} (A)	4.25	4.26	1.28
V_{mp} (V)	33	17.6	15.6
P_{maxe} (W)	140.2	75	20
β_i (mA/°C)	2	2	0.2
β_v (mV/°C)	-152	-76	-100
N_s	72	36	42
V_{NOCT} (V)	39.2	20.0	20.2
T_{NOCT} (°C)	47	45	45

according to the datasheet information provided by the manufacturer using the analytical and iterative approach, so the parameters I_{pv} , I_s and A are calculated through Eqs. (5), (10) and (16), respectively. But the

Table 7

The experimental and estimated values and the corresponding Individual Absolute Error of the V_{oc} for Shell SP140 Module.

T (°C)	Experimental V_{oc} (V)	Estimated V_{oc} (V)	IAE_{Voc} (V)	G (W/m ²)	Experimental V_{oc} (V)	Estimated V_{oc} (V)	IAE_{Voc} (V)
20	43,47238	43.5828	0,11042	1000	42,8956	43,0071	0.1115
30	41,94444	42.0628	0,11836	800	42,2544	42,3000	0.0456
40	40,625	40.5428	0,0822	600	41,4031	41,5823	0.1792
50	39,09722	39.0228	0,07442	400	40,2912	40,3071	0.0159
60	37,70833	37.5028	0,20553	200	38,2751	38,4428	0.1677

series and shunt resistances are estimated using an iterative method. Then all model parameters, all five parameters are calculated using our model for three photovoltaic modules Shell SP140, Shell S75 and Shell ST20 are summarized in Table 8

Eq. (2), Eq. (31) and Eq. (32) are used to plotting the Current-Voltage characteristic curve of the actual output for photovoltaic modules.

The performance of proposed approach is validated for the Photovoltaic module of three different technologies such as mono-crystalline (Shell SP140), poly-crystalline (Shell S75) and thin film (Shell ST20). The accuracy of proposed model with respect to the experimental data is studied using the Current-Voltage and Power-Voltage curves for an incident irradiance $G = 1000 \text{ W/m}^2$ and different values of module temperature T , and also for module temperature $T = 25 \text{ }^\circ\text{C}$ and different value of incident irradiance G for previous three modules are shows in the Figs. 7–11. All these figures show that every point in the simulated I-V and P-V curves are in accordance with experimental values, i.e the theoretical and simulated curves is almost merged. Thus there is a good correlation between the results obtained by our model and the values given by the manufacturer. Finally, we can conclude from all these figures that our proposed model is successfully validated under different environmental conditions and confirms the accuracy of the extraction procedure.

More accurate performance evaluation

In this paragraph another complementary method was adopted in order to obtain a more accurate evaluation of the performance of our result obtained in previous section, we proposed to calculate the Average Relative Error (ARE) and the Root Mean Square Error (RMSE), then we compared the obtained value using the proposed method with villalva's [67]and kashif's models [71]. Several methods have been developed to calculate ARE, each of these methods involves a slightly different statistical calculation (Shaw, 1997; Long, 1998; Stanley, 1999). Since these measurement error estimates are calculated using different formulas [74], in our study we will use the following relationship[64]:

$$ARE = \frac{1}{N} \sum_{i=1}^N \frac{|I_{i,estimated} - I_{i,experimental}|}{I_{i,experimental}} \quad (35)$$

$$RMSE = \sqrt{\frac{\sum_{i=1}^N (I_{i,experimental} - I_{i,estimated})^2}{N}} \quad (36)$$

where $I_{i,estimated}$, $I_{i,experimental}$, N are the estimated current, experimental current, number of the estimated or experimental current, respectively.

Irradiation change and temperature constant

When G changes and $T = 25 \text{ }^\circ\text{C}$, Table 9 shows the obtained values of Average Relative Errors (ARE) of three different models. Fig. 12(a) and (b) shows their variation at different level of irradiation G for Shell SP 140 and for Shell S75 PV modules. It can be seen that ARE of the Kashif's model [71] is the largest, with a maximum value of 62.61 % for S75 module at $G = 400 \text{ W/m}^2$. For PV module Shell SP140, Shell S75, the obtained values of ARE with kashif's model are significantly greater than that of the proposed model and Villalva's model. In addition, for two PV modules, the performance of the Villalva's model is not very different from that of the proposed model because in our study we are

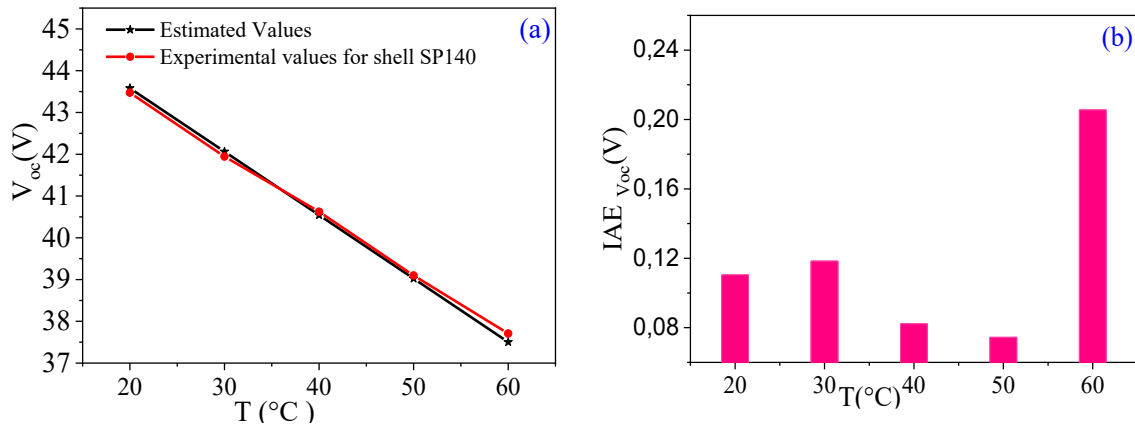


Fig. 5. Variation of the Estimated and Experimental values of V_{oc} vs T for Shell SP140 module when $G = 1000 \text{ (W/m}^2\text{)}$: (a), Individual Absolute Errors of V_{oc} (b).

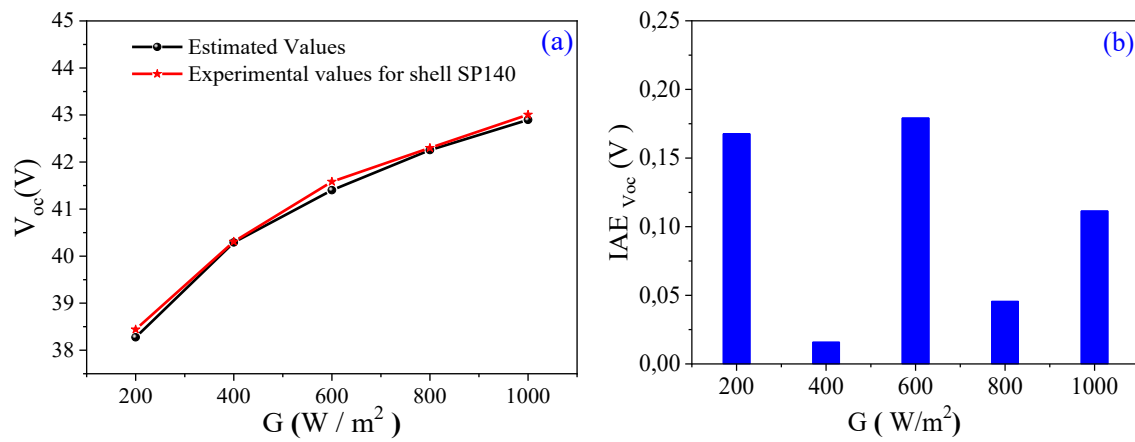


Fig. 6. Variation of the Estimated and Experimental values of V_{oc} vs G for Shell SP140 module when $T = 25 \text{ }^\circ\text{C}$ (a), Individual Absolute Errors of V_{oc} (b).

Table 8

Calculated model parameters of the proposed approach compared with Villalva's method [67] and Gang Wang's method [73].

PV modules	A	$I_{pv}(A)$	$I_s (A)$	$R_s(\Omega)$	$R_p(\Omega)$
Shell SP140	1.2714	4.7148	$5.694 \cdot 10^{-8}$	0.8540	272.9720
Shell S75	1.5	4.7025	$7.915 \cdot 10^{-7}$	0.086	164.1287
Shell ST20	2.9071	1.54	$1.022 \cdot 10^{-3}$	1.342	$1.58 \cdot 10^5$

using the same approach adopted in [67]. Also, in most cases, the performance of the proposed approach can be closed to or better than that of the villalva's model with a minimum value of 1.14 % for SP140 at $G = 100 \text{ W/m}^2$ and $T = 25 \text{ }^\circ\text{C}$.

Temperature changes and irradiation constant:

When T changes and $G = 1000 \text{ W/m}^2$, Table 10 shows the ARE of three different models. Fig. 13(a), (b) and Fig. 14 show their variation at different level of temperature T for Shell SP 140, Shell S75 and Shell

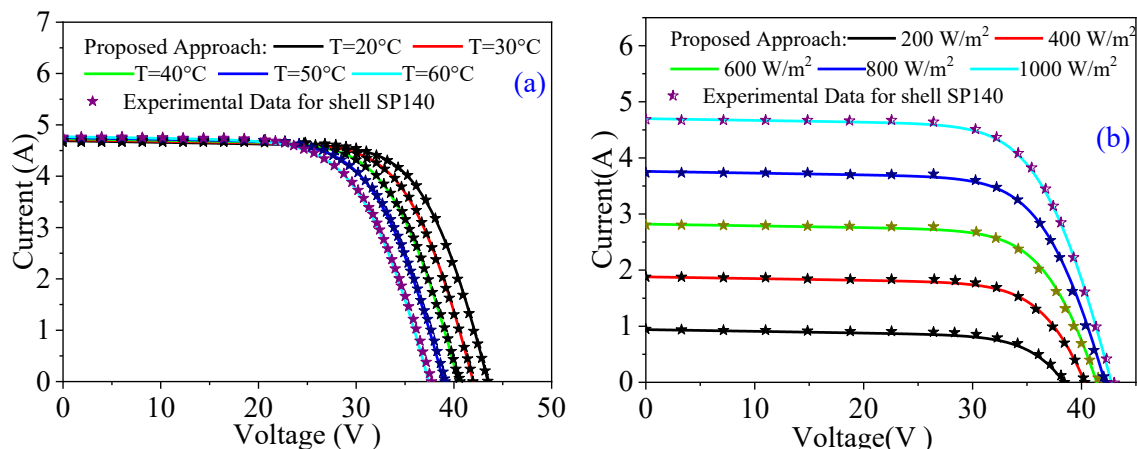


Fig. 7. I-V curves of proposed model of the shell SP140 PV module for several temperature (a) and Irradiation levels (b).

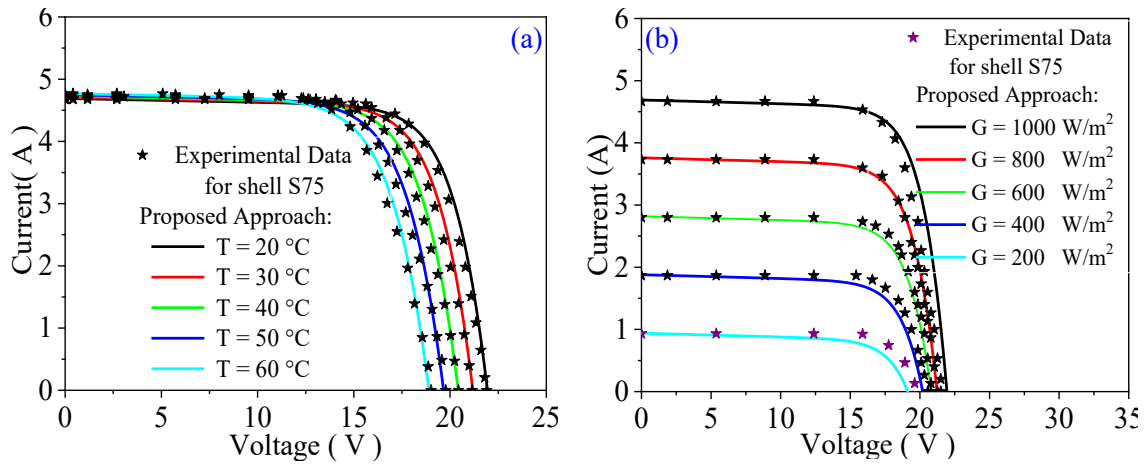


Fig. 8. I-V curves of proposed model of the shell S75 PV module for several temperature (a) and Irradiation levels (b).

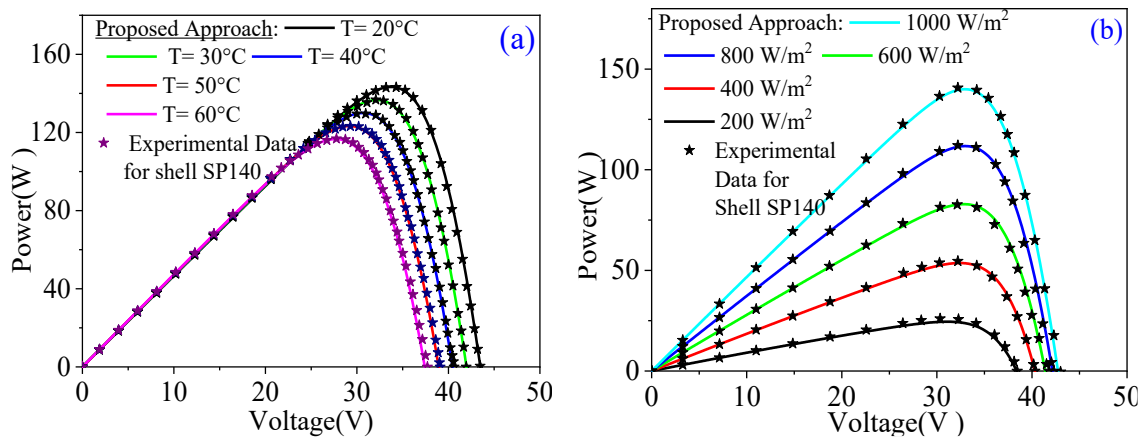


Fig. 9. P-V curves of proposed model of the shell SP140 PV module for several temperature (a) and Irradiation levels (b).

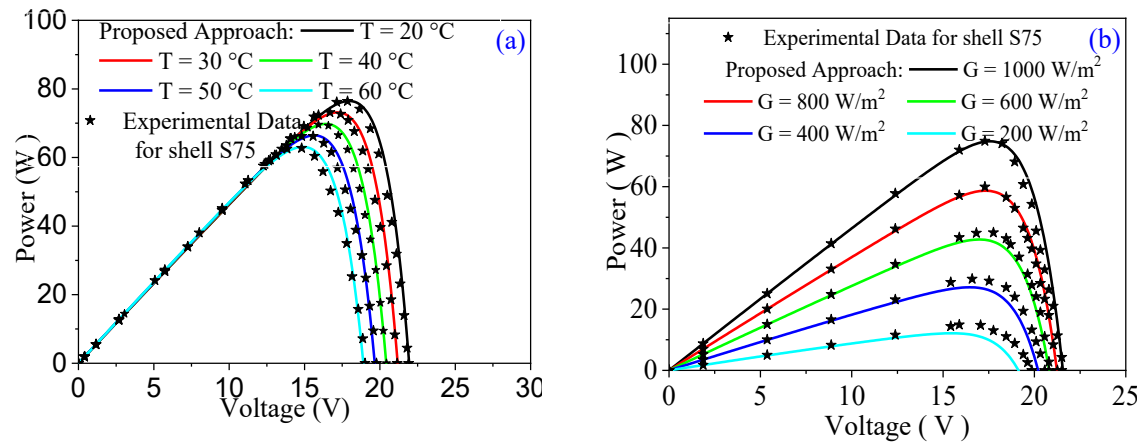


Fig. 10. P-V curves of proposed model of the shell S75 PV module for several temperature (a) and Irradiation levels (b).

ST20 PV modules. It can be seen that the ARE of the kashif's model are still large, and the maximum value can reach 38.54 % using Shell ST20 PV module. Also, from Table 6 we can see for these three different PV modules at different temperatures, the performance of the proposed approach can be closed to the Villalva's model, thus verifying the effectiveness of the proposed model.

Evaluation at standard test conditions

In this section we use for evaluate our model the polycrystalline Module used in [75]. Fig. 15 show the obtained both estimated and experimental data points I-V and P-V curves for polycrystalline PV modules compared with different model such as Y.Tao's Model[75], S. Shongwe's Model [76], W.De Soto's Model [65] and Phang's Model [77]. an excellent agreement between the I-V and P-V points are

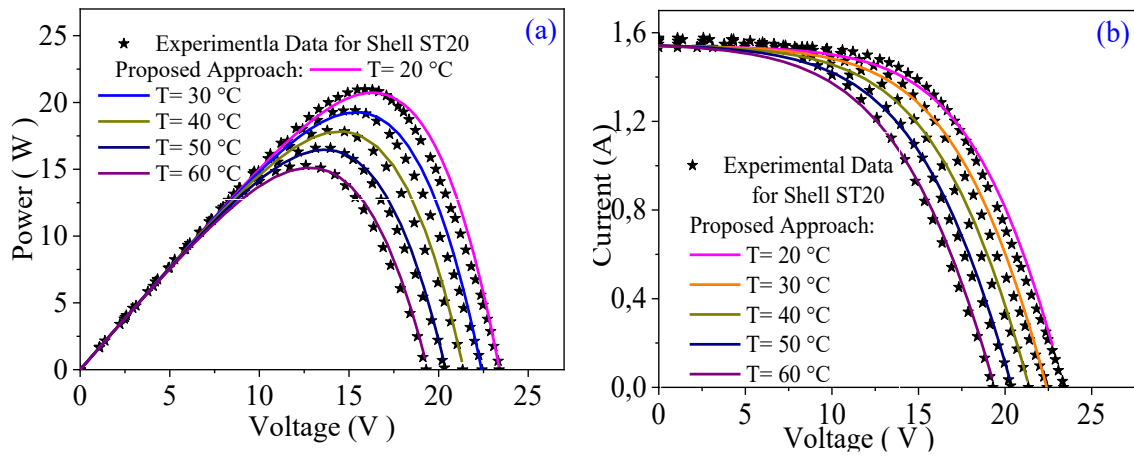


Fig. 11. P-V (a) and I-V (b) curves of proposed model of the shell ST20 PV module for several temperature levels.

Table 9
Comparison of Average Relative Errors (ARE) when Temperature T = 25 °C.

PV modules	G(W/m ²)	K. Ishaque's model (%)	Villalva's model (%)	Proposed model (%)
SP140	1000	10.79	4.26	1.14
	800	15.08	4.57	2.08
	600	18.95	7.33	2.97
	400	12.85	6.12	3.60
	200	19.39	5.65	3.36
S75	1000	54.79	38.93	25.82
	800	46.39	16.84	15.64
	600	58.20	15.41	18.73
	400	62.61	20.81	19.28
	200	47.23	19.60	21.41

determined using the proposed model and its better than those obtained using other model, but we can observe a small difference between measured and estimated value for Phang's model in MPP point.

Table 11 summarized the calculated values of all model parameters and RMSE compared with previously model. It can be see that the minimum value of RMSE is **0.0031 A** obtained with the proposed model, this result indicates that the estimated values using our model are very close to the experimental data at STCs. Also, we are introduced the IAE for our model compared with previously model and its variation are shown in Fig. 16, from this figure we can see that the IAE of our model almost have the same variation as the Y.Tao's Model, W.De Soto's Model

and Phang's Model. Also, the minimum value of IAE is equal to zero with Y.Tao's model at the vicinity of voltage V = 39 V.

Advantage and disadvantages of the proposed model.

Compared with the others approach and with Artificial intelligence algorithms that require a few input data and use powerful mathematical tools for estimated all model parameter accurately but at long calculation time. The advantages of our model based on hybrid approach are:

- All estimated parameter model investigated in this study attempts to use the available data to accurately predict energy production;
- Applicable in large-scale PV systems especially for three PV technologies like monocrystalline, polycrystalline and the thin films PV cells/modules;
- Using a Processor Intel(R)Core(TM)i5-6500 CPU @3.2 GHz 3.19 GHz; RAM:8.00G, the obtained computation time is 0.23 s that lower than those obtained using others model (Y.Tao's model, S. Shongwe's model, W.De Soto's model and Phang's Model).
- The accuracy of proposed model is high compared with previously approach;

The disadvantages of proposed model are:

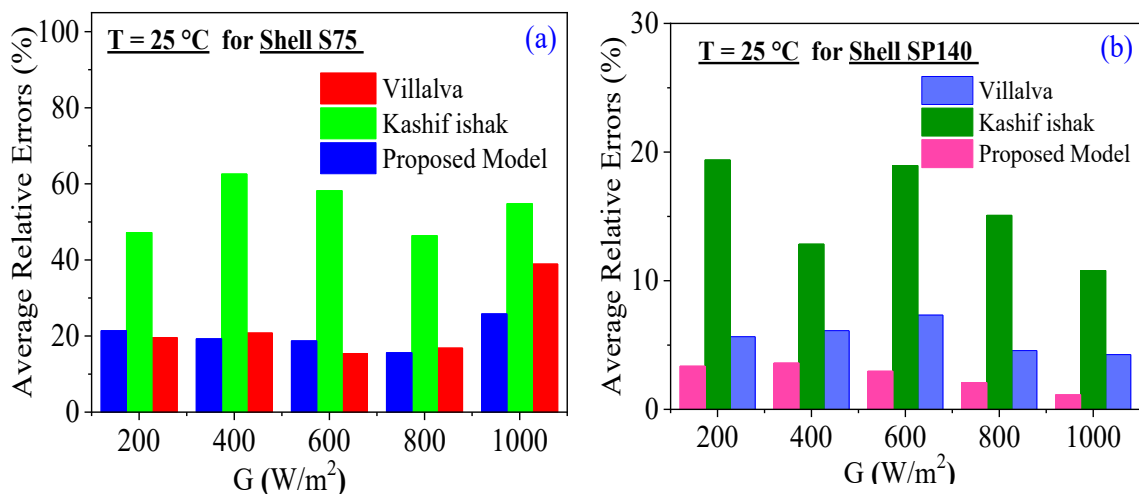


Fig. 12. ARE of three different models when G changes and T = 25 °C, for Shell S75 (a); and for Shell SP 140(b).

Table 10
Comparison of Average Relative Errors (ARE) when Irradiance $G = 1000 \text{ W/m}^2$.

PV module	T °C	K. Ishaque's model (%)	Villalva's model (%)	Proposed model (%)
SP140	20	31.67	2.70	2.41
	30	9.76	3.69	2.70
	40	8.34	5.97	3.32
	50	6.86	6.78	3.56
	60	7.60	7.19	4.47
S75	20	14.01	4.88	3.15
	30	8.14	5.51	4.36
	40	6.49	5.91	4.75
	50	5.84	6.81	4.58
	60	7.21	7.79	5.43
ST20	20	38.54	8.08	7.76
	30	8.78	9.44	7.32
	40	6.52	7.08	7.78
	50	11.89	9.87	8.47
	60	8.63	10.09	8.31

- In the construction step the performance of our model was tested with a large amount of PV modules and it was remarked that the proposed model is not valid for all PV systems;
- Requires a large amount of input data.

Conclusion

In this study, a new Hybrid approach is introduced to estimate the parameters of solar cells and photovoltaic modules or panels. This approach is based on two main steps, the first is purely analytical and the second is iterative approach that is implemented in Matlab using for calculated the series and shunt resistance. The method then is used to find the best configuration to the parameters of and Photovoltaic modules using RMSE and ARE as criteria. In order to analyze the performance and stability, our approach has been tested using data provided by the manufacturers for Shell SP140, S75 and ST20 modules. The obtained results of the proposed approach have been compared with others models such as K. Ishaque's model and Villalva's model to estimate the parameters of previously Photovoltaic modules. Moreover, the I-V and P-V curves indicate a good correlation between the estimated values using our model and the values given by the manufacturer. When G changes, the minimum values of ARE is equal to 1.41% and when T changes the minimum value is equal to 2.41%, these two values are obtained using our approach. From these results, it can be concluded that the performance of our model is close to the results of Villalva's model for estimating the parameters of Single diode model, and even it is

better than the K. Ishaque's model. An additional test has been performed to verify the stability of the proposed Approach. In this test, the proposed approach is compared with Y.Tao's model, S. Shongwe's model, Phang's model and W.De Soto's model. The obtained RMSE using our approach is 0.0031 A, it's considered as the smallest among the values found by the compared models. The computation time is 0.23 s lower than those obtained using previously approach. Also, the IAE is calculated and it's very low in the voltage range [0, 30 V] compared with the others model, it takes a minimum value equal to 0.00191 at the vicinity of $V = 37 \text{ V}$. All estimated outcomes provide evidence that the obtained values by our model are better and outperforms all previously compared models under dynamic test conditions. Furthermore, the parameter extraction method is superior in terms of accuracy and convergence. The possible directions for future work would be (i) the implementation of the model in practical applications; (ii) modeling of the dynamic optimization techniques and application for tracking the global MPP; (iii) the employment of the dynamic optimization techniques in other applications such as control systems and power electronics.

CRedit authorship contribution statement

Dris Ben hmamou: Conceptualization, Validation, Writing –

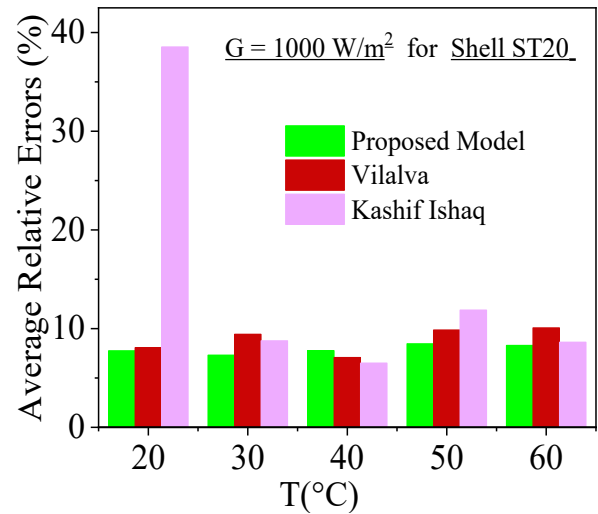


Fig. 14. ARE for Shell ST20 when T changes, $G = 1000 \text{ W/m}^2$.

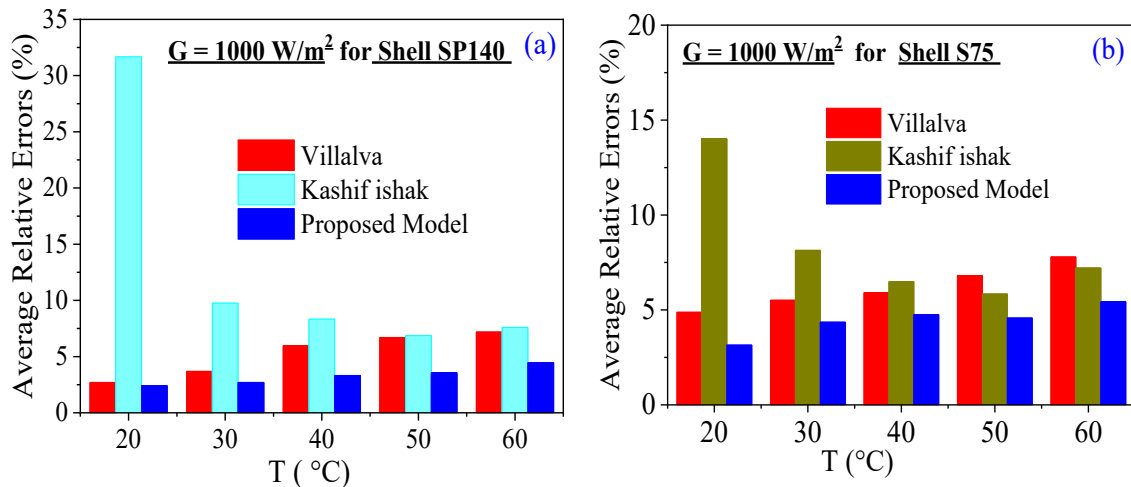


Fig. 13. ARE of three different models when T changes and $G = 1000 \text{ W/m}^2$, for Shell SP 140 (a); and for Shell S75 (b).

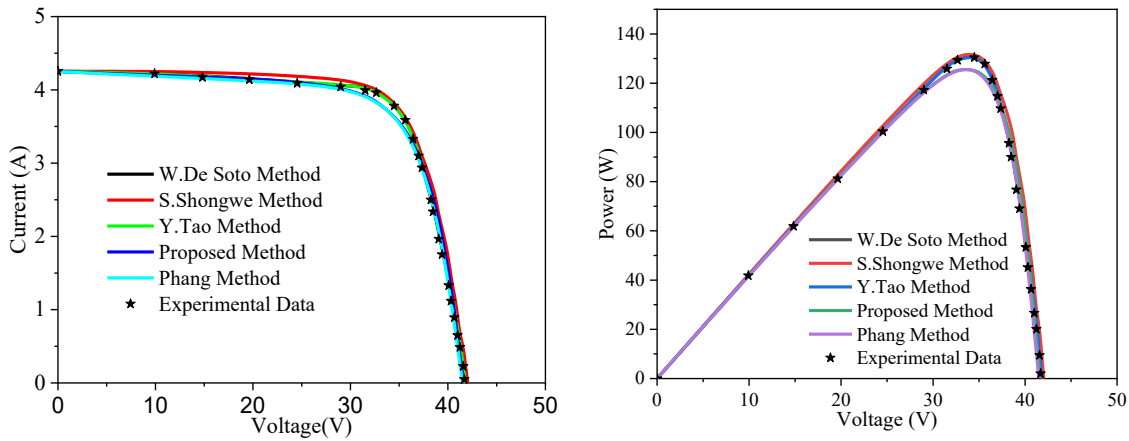


Fig. 15. Measured and simulated I-V and P-V curves for polycrystalline PV modules at STCs.

Table 11
Comparison of calculated Root Mean Square Error (RMSE) at STCs.

Parameters	Polycrystalline PV Module				
	Y.Tao	S. Shongwe	Phang	W.De Soto	Proposed method
$I_{pv}(A)$	4.285	4.253	4.253	4.270	4.250
$I_o(A)$	$1.36 \cdot 10^{-9}$	$3.54 \cdot 10^{-6}$	$2.85 \cdot 10^{-11}$	$1.28 \cdot 10^{-10}$	$7.45 \cdot 10^{-6}$
A	1.904	2.968	1.500	1.718	1.710
$R_c(\Omega)$	0.823	0.319	0.1235	0.919	0.0020
$R_p(\Omega)$	155.850	411.948	155.85	148.89	199.1565
RMSE(A)	0.00431	0.01359	0.054	0.0232	0.0031
Computation time(s)	0.83	0.7	0.41	0.57	0.23

Daoudi El fatmi: Investigation, Writing – review & editing. **Sergey Obukhov:** Investigation, Writing – review & editing.

Declaration of Competing Interest

The authors declare that they have no known competing financial interests or personal relationships that could have appeared to influence the work reported in this paper.

Acknowledgments

This research was supported by Faculty of Sciences of Agadir Ibn Zohr University.

Also, this research was supported by Tomsk polytechnic university development program.

References

- [1] Yahya-Khotbehsara A, Shakhoseini A. A fast modeling of the double-diode model for PV modules using combined analytical and numerical approach. *Sol Energy* 2018;162(January):403–9. <https://doi.org/10.1016/j.solener.2018.01.047>.
- [2] Streimikiene D, Girdzijauskas S. Assessment of post-Kyoto climate change mitigation regimes impact on sustainable development. *Renew Sustain Energy Rev* 2009;13(1):129–41. <https://doi.org/10.1016/j.rser.2007.07.002>.
- [3] Lau LC, Teong K, Mohamed AR. Global warming mitigation and renewable energy policy development from the Kyoto Protocol to the Copenhagen Accord — A comment. *Renew Sustain Energy Rev* 2012;16(7):5280–4. <https://doi.org/10.1016/j.rser.2012.04.006>.
- [4] Zhang C, Xu T, Feng H, Chen S. Greenhouse gas emissions from landfills: A review and bibliometric analysis. *Sustain.* 2019;11(8):1–15. <https://doi.org/10.3390/su11082282>.
- [5] Jha SK, Bilalovic J, Jha A, Patel N, Zhang H. Renewable energy: present research and future scope of Artificial Intelligence. *Renew Sustain Energy Rev* 2017;77 (April):297–317. <https://doi.org/10.1016/j.rser.2017.04.018>.
- [6] Baghdadi F, Mohammedi K, Diaf S, Behar O. Feasibility study and energy conversion analysis of stand-alone hybrid renewable energy system. *Energy Convers Manag* 2015;105:471–9. <https://doi.org/10.1016/j.enconman.2015.07.051>.
- [7] Ben Hmamou D, Elyaqouti M, Arjdal E, Chaoufi J, Saadaoui D, Lidaighbi S, et al. Particle swarm optimization approach to determine all parameters of the photovoltaic cell. *Mater Today: Proc* 2022;52:7–12. <https://doi.org/10.1016/j.matpr.2021.10.083>.
- [8] Sheraz Khalid M, Abido MA. A novel and accurate photovoltaic simulator based on seven-parameter model. *Electr Power Syst Res* 2014;116:243–51. <https://doi.org/10.1016/j.epr.2014.06.010>.
- [9] Chin VJ, Salam Z, Ishaque K. Cell modelling and model parameters estimation techniques for photovoltaic simulator application: A review. *Appl Energy* 2015; 154:500–19. <https://doi.org/10.1016/j.apenergy.2015.05.035>.
- [10] Khanna V, Das BK, Bisht D, Vandana, Singh PK. A three diode model for industrial solar cells and estimation of solar cell parameters using PSO algorithm. *Renew Energy* 2015;78:105–13. <https://doi.org/10.1016/j.renene.2014.12.072>.
- [11] Lo Brano V, Orioli A, Ciulla G, Di Gangi A. An improved five-parameter model for photovoltaic modules. *Sol Energy Mater Sol Cells* 2010;94(8):1358–70. <https://doi.org/10.1016/j.solmat.2010.04.003>.

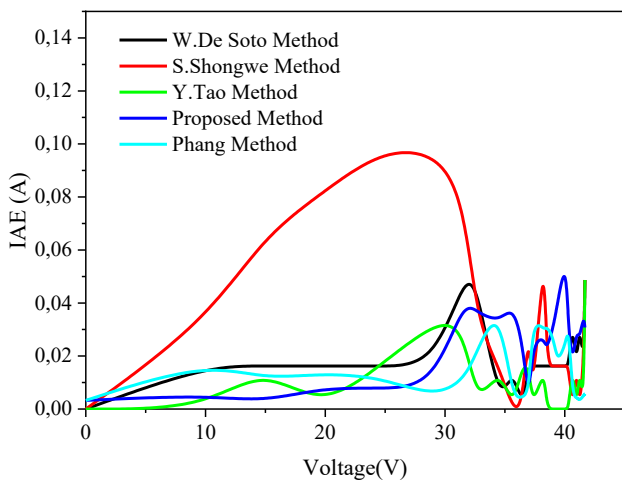


Fig. 16. The obtained IAE for Polycrystalline Module at STCs.

original draft, Writing – review & editing. **Mustapha Elyaqouti:** Conceptualization, Validation, Writing – original draft, Writing – review & editing. **El hanafi Arjdal:** Conceptualization, Validation, Writing – original draft, Writing – review & editing. **Driss Saadaoui:** Conceptualization, Methodology, Writing – review & editing, Software, Formal analysis, Funding acquisition. **Soud Lidaighbi:** Conceptualization, Methodology, Writing – review & editing, Software, Formal analysis, Funding acquisition. **Jamal Chaoufi:** Conceptualization, Validation, Writing – original draft, Writing – review & editing. **Ahmed Ibrahim:** Conceptualization, Validation, Writing – original draft, Writing – review & editing. **Rabya Aqel:** Investigation, Writing – review & editing.

- [12] Sheraz M, Abido MA, "An efficient approach for parameter estimation of PV model using de and fuzzy based MPPT controller," *2014 IEEE Conf. Evol. Adapt. Intell. Syst. EAIS 2014 - Conf. Proc.*, 2014, doi: 10.1109/eaiss.2014.6867487.
- [13] Zagrouba M, Sellami A, Bouaicha M, Ksouri M. Identification of PV solar cells and modules parameters using the genetic algorithms: Application to maximum power extraction. *Sol Energy* 2010;84(5):860–6. <https://doi.org/10.1016/j.solener.2010.02.012>.
- [14] Saadaoui D, Elyaqouti M, Assalou K, Ben hmamou D, Lidaighbi S. Parameters optimization of solar PV cell/module using genetic algorithm based on non-uniform mutation. *Energy Convers Manag X* 2021;12:100129. <https://doi.org/10.1016/j.ecmx.2021.100129>.
- [15] Ketkar M, Chopde AM. Efficient parameter extraction of solar cell using modified ABC. *Int J Comput Appl* 2014;102(1):1–6. <https://doi.org/10.5120/17776-8535>.
- [16] Awadallah MA, Venkatesh B. Bacterial Foraging Algorithm Guided by Particle Swarm Optimization for Parameter Identification of Photovoltaic Modules. *Can J Electr Comput Eng* 2016;39(2):150–7.
- [17] Jacob B, Balasubramanian K, Babu TS, Rajasekar N. Parameter extraction of solar PV double diode model using artificial immune system. In: 2015 IEEE Int Conf. Signal Process. Informatics, Commun. Energy Syst. SPICES 2015; 2015. <https://doi.org/10.1109/SPICES.2015.7091390>.
- [18] Mirbagheri SM, Mirbagheri SZ, Mokhlis H, "Stand-alone hybrid renewable energy system simulation and optimization using imperialist competitive algorithm," In *POWERCON 2014 - 2014 Int. Conf. Power Syst. Technol. Towar. Green, Effic. Smart Power Syst. Proc.*, no. Powercon, pp. 1127–1134, 2014, doi: 10.1109/POWERCON.2014.6993983.
- [19] Kharchouf Y, Herbazi R, Chahboun A. Parameter's extraction of solar photovoltaic models using an improved differential evolution algorithm. *Energy Convers Manag* 2022;251(October):114972. <https://doi.org/10.1016/j.enconman.2021.114972>.
- [20] Dali A, Bouharchouche A, Diaf S. Parameter identification of photovoltaic cell/module using genetic algorithm (GA) and particle swarm optimization (PSO). In: 3rd Int Conf. Control. Eng. Inf. Technol. CEIT; 2015. <https://doi.org/10.1109/CEIT.2015.7233137>.
- [21] Dehghani M, Taghipour M, Gharehpetian GB, Abedi M, "Optimized Fuzzy Controller for MPPT of Grid-connected PV Systems in Rapidly," vol. 9, no. 2, pp. 376–383, doi: 10.35833/MPCE.2019.000086.
- [22] Bahrani P, Jain N, "Performance Analysis of P&O and FLC Method of MPPT for PV Module Based on Five-Parameter Model," 2022, pp. 357–369.
- [23] Madeti SR, Singh SN. Modeling of PV system based on experimental data for fault detection using kNN method. *Sol Energy* 2018;173(March):139–51. <https://doi.org/10.1016/j.solener.2018.07.038>.
- [24] Zhu H, Lu L, Yao J, Dai S, Hu Y. Fault diagnosis approach for photovoltaic arrays based on unsupervised sample clustering and probabilistic neural network model. *Sol Energy* 2018;176(October):395–405. <https://doi.org/10.1016/j.solener.2018.10.054>.
- [25] Douiri MR. Particle swarm optimized neuro-fuzzy system for photovoltaic power forecasting model. *Sol Energy* 2019;184(March):91–104. <https://doi.org/10.1016/j.solener.2019.03.098>.
- [26] Bök H, Poikonen A, Aarva A, Mielonen T, Pitkänen MRA, Lindfors AV. Photovoltaic system modeling: A validation study at high latitudes with implementation of a novel DNI quality control method. *Sol Energy* 2020;204(April):316–29. <https://doi.org/10.1016/j.solener.2020.04.068>.
- [27] Li B, Delpha C, Diallo D, Migan-Dubois A. Application of Artificial Neural Networks to photovoltaic fault detection and diagnosis: A review. *Renew Sustain Energy Rev* 2019;138(December):2021. <https://doi.org/10.1016/j.rser.2020.110512>.
- [28] Lidaighbi S, Elyaqouti M, Assalou K, Ben Hmamou D, Saadaoui D, H'roua J. Parameter estimation of photovoltaic modules using analytical and numerical/iterative approaches: A comparative study. *Mater Today: Proc* 2022;52:1–6.
- [29] Louzani M, Khouya A, Al-Dahidi S, Mussetta M, Amechnou K. Analytical optimization of photovoltaic output with Lagrange Multiplier Method. *Optik (Stuttg)* 2019;199:163379. <https://doi.org/10.1016/j.ijleo.2019.163379>.
- [30] Qais MH, Hasanien HM, Alghuwainem S. Identification of electrical parameters for three-diode photovoltaic model using analytical and sunflower optimization algorithm. *Appl Energy* 2019;250(January):109–17. <https://doi.org/10.1016/j.apenergy.2019.05.013>.
- [31] Toledo FJ, Blanes JM. Analytical and quasi-explicit four arbitrary point method for extraction of solar cell single-diode model parameters. *Renew Energy* 2016;92:346–56. <https://doi.org/10.1016/j.renene.2016.02.012>.
- [32] Ruschel CS, Gasparin FP, Costa ER, Krenzinger A. Assessment of PV modules shunt resistance dependence on solar irradiance. *Sol Energy* 2016;133:35–43. <https://doi.org/10.1016/j.solener.2016.03.047>.
- [33] Tong NT, Pora W. A parameter extraction technique exploiting intrinsic properties of solar cells. *Appl Energy* 2016;176:104–15. <https://doi.org/10.1016/j.apenergy.2016.05.064>.
- [34] Bogning Dongue S, Njomo D, Ebengai L. An improved nonlinear five-point model for photovoltaic modules. *Int J Photoenergy* 2013;2013:1–11.
- [35] Deihimi MH, Naghizadeh RA, Meyabadi AF. Systematic derivation of parameters of one exponential model for photovoltaic modules using numerical information of data sheet. *Renew Energy* 2016;87:676–85. <https://doi.org/10.1016/j.renene.2015.10.066>.
- [36] Laudani A, Lozito GM, Mancilla-David F, Riganti-Fulginei F, Salvini A. An improved method for SRC parameter estimation for the CEC PV module model. *Sol Energy* 2015;120:525–35. <https://doi.org/10.1016/j.solener.2015.08.003>.
- [37] Batzelis EI, Member S, Papatthaniou SA, Member S, "A Method for the Analytical Extraction of the Single-Diode PV Model Parameters," pp. 1–9, 2015.
- [38] Silva EA, Bradaschia F, Cavalcanti MC, Nascimento AJ. Parameter estimation method to improve the accuracy of photovoltaic electrical model. *IEEE J Photovoltaics* 2016;6(1):278–85. <https://doi.org/10.1109/JPHOTOV.2015.2483369>.
- [39] Laudani A, Riganti Fulginei F, Salvini A. Identification of the one-diode model for photovoltaic modules from datasheet values. *Sol Energy* 2014;108:432–46. <https://doi.org/10.1016/j.solener.2014.07.024>.
- [40] Zaimi M, El Achouby H, Ibral A, Assaid EM. Determining combined effects of solar radiation and panel junction temperature on all model-parameters to forecast peak power and photovoltaic yield of solar panel under non-standard conditions. *Sol Energy* 2019;191(July):341–59. <https://doi.org/10.1016/j.solener.2019.09.007>.
- [41] Tutkun N, Elibol E, Aktas M. Parameter extraction from a typical PV module using a metaheuristic technique. In: 2015 Int Conf. Renew. Energy Res. Appl. ICRERA; 2015. p. 755–9. <https://doi.org/10.1109/ICRERA.2015.7418512>.
- [42] Fébba DM, Rubinger RM, Oliveira AF, Bortoni EC. Impacts of temperature and irradiance on polycrystalline silicon solar cells parameters. *Sol Energy* 2018;174(September):628–39. <https://doi.org/10.1016/j.solener.2018.09.051>.
- [43] Ghani F, Rosengarten G, Duke M, Carson JK. On the influence of temperature on crystalline silicon solar cell characterisation parameters. *Sol Energy* 2015;112:437–45. <https://doi.org/10.1016/j.solener.2014.12.018>.
- [44] Khan F, Baek SH, Kim JH. Wide range temperature dependence of analytical photovoltaic cell parameters for silicon solar cells under high illumination conditions. *Appl Energy* 2016;183:715–24. <https://doi.org/10.1016/j.apenergy.2016.09.020>.
- [45] Singh P, Ravindra NM. Temperature dependence of solar cell performance - An analysis. *Sol Energy Mater Sol Cells* 2012;101:36–45. <https://doi.org/10.1016/j.solmat.2012.02.019>.
- [46] Khan F, Singh SN, Husain M. Effect of illumination intensity on cell parameters of a silicon solar cell. *Sol Energy Mater Sol Cells* 2010;94(9):1473–6. <https://doi.org/10.1016/j.solmat.2010.03.018>.
- [47] Khan F, Baek SH, Park Y, Kim JH. Extraction of diode parameters of silicon solar cells under high illumination conditions. *Energy Convers. Manag.* 2013;76:421–9. <https://doi.org/10.1016/j.enconman.2013.07.054>.
- [48] Chegaar M, Hamzaoui A, Namoda A, Petit P, Aillerie M, Herguth A. Effect of illumination intensity on solar cells parameters. *Energy Procedia* 2013;36:722–9. <https://doi.org/10.1016/j.egypro.2013.07.084>.
- [49] Khan F, Baek SH, Kim JH. Intensity dependency of photovoltaic cell parameters under high illumination conditions: An analysis. *Appl Energy* 2014;133(August):356–62. <https://doi.org/10.1016/j.apenergy.2014.07.107>.
- [50] Cuce E, Cuce PM, Bali T. An experimental analysis of illumination intensity and temperature dependency of photovoltaic cell parameters. *Appl Energy* 2013;111:374–82. <https://doi.org/10.1016/j.apenergy.2013.05.025>.
- [51] Deshmukh MP, Nagaraju J. Measurement of silicon and GaAs/Ge solar cell device parameters. *Sol Energy Mater Sol Cells* 2005;89(4):403–8. <https://doi.org/10.1016/j.solmat.2005.01.005>.
- [52] Singh P, Singh SN, Lal M, Husain M. Temperature dependence of I-V characteristics and performance parameters of silicon solar cell. *Sol Energy Mater Sol Cells* 2008;92(12):1611–6. <https://doi.org/10.1016/j.solmat.2008.07.010>.
- [53] Ding J, Cheng X, Fu T. Analysis of series resistance and P-T characteristics of the solar cell. *Vacuum* 2005;77(2):163–7. <https://doi.org/10.1016/j.vacuum.2004.08.019>.
- [54] Arora JD, Verma AV, Bhatnagar M. Variation of series resistance with temperature and illumination level in diffused junction poly- and single-crystalline silicon solar cells. *J Mater Sci Lett* 1986;5(12):1210–2. <https://doi.org/10.1007/BF01729367>.
- [55] Eikelboom JA, Reinders A, "Determination of the irradiation dependent efficiency of Multicrystalline Si PV modules on basis of I-V Curve fitting and its influence on the annual performance," In *14-th Eur. PV Sol. Energy Conf. July*, pp. 293–296. URL <ftp://kerntechnik.nl/pub/www/library/report/1997/rx97045.pdf>, vol. 81, no. 922, pp. 235–236, 1965, doi: 10.2473/shigentosozai1953.81.922.235.
- [56] Lim LHI, Ye Z, Ye J, Yang D, Du H. A linear method to extract diode model parameters of solar panels from a single I-V curve. *Renew. Energy* 2015;76:135–42. <https://doi.org/10.1016/j.renene.2014.11.018>.
- [57] Banerjee S, Anderson WA. Temperature dependence of shunt resistance in photovoltaic devices. *Appl Phys Lett* 1986;49(1):38–40. <https://doi.org/10.1063/1.97076>.
- [58] Priyanka, Lal M, Singh SN. A new method of determination of series and shunt resistances of silicon solar cells. *Sol Energy Mater Sol Cells* 2007;91(2-3):137–42. <https://doi.org/10.1016/j.solmat.2006.07.008>.
- [59] S. Sp-pc, "Product Information Sheet Shell SP140-PC Module Shell SP140-PC Typical I / V Characteristics".
- [60] Renewables-Energy, "© 2002 Shell International Renewables," 1999.
- [61] Walker G, "EVALUATING MPPT CONVERTER TOPOLOGIES USING A MATLAB PV MODEL," no. January 2001, 2014.
- [62] CHIH-TANG SAH, ROBERT N. NOYCE, WILLIAMSHOCKLEY, "Carrier Generation and Recombination in P-NV Junctions and P-N Junction Characteristics," vol. 1, 1956.
- [63] Alrashidi MR, "Heuristic Approach for Estimating the Solar Cell Parameters," pp. 80–83.
- [64] Shinong W, Qianlong M, Jie X, Yuan G, Shilin L. An improved mathematical model of photovoltaic cells based on datasheet information. *Sol Energy* 2020;199(February):437–46. <https://doi.org/10.1016/j.solener.2020.02.046>.
- [65] De Soto W, Klein SA, Beckman WA, "Improvement and validation of a model for photovoltaic array performance," vol. 80, pp. 78–88, 2006, doi: 10.1016/j.solener.2005.06.010.
- [66] Kou Q, Klein SA, Beckman WA, "A method for estimating the long-term performance of direct-coupled pv pumping systems," vol. 64, no. 98, pp. 33–40, 1998.

- [67] Villalva MG, Gazoli JR, Filho ER, "Comprehensive Approach to Modeling and Simulation of Photovoltaic Arrays," vol. 24, no. 5, pp. 1198–1208, 2009.
- [68] Hussein KH, Osakada M, "Maximum photovoltaic power tracking : an algorithm for rapidly changing atmospheric conditions," pp. 59–64.
- [69] González-longatt FM, "Model of Photovoltaic Module in Matlab™," pp. 1–5, 2005.
- [70] Carrero C, Amador J, Arnaltes S, "A single procedure for helping PV designers to select silicon PV modules and evaluate the loss resistances," vol. 32, pp. 2579–2589, 2007, doi: 10.1016/j.renene.2007.01.001.
- [71] Ishaque K, Salam Z, Taheri H, Syafaruddin. Simulation Modelling Practice and Theory Modeling and simulation of photovoltaic (PV) system during partial shading based on a two-diode model. Stimul Model Pract THEORY 2011;19(7): 1613–26. <https://doi.org/10.1016/j.simpat.2011.04.005>.
- [72] Stormelli V, Muttillio M, De Rubeis T, Nardi I, "A New Simplified Five-Parameter Estimation Method for Single-Diode Model of Photovoltaic Panels," pp. 1–20, 2019, doi: 10.3390/en12224271.
- [73] Wang G, Zhao Ke, Shi J, Chen W, Zhang H, Yang X, et al. An iterative approach for modeling photovoltaic modules without implicit equations. Appl Energy 2017;202: 189–98. <https://doi.org/10.1016/j.apenergy.2017.05.149>.
- [74] Clifford Stanley and Lawie Dave, "Average Relative Error in Geochemical Determinations: Clarification, Calculation, and a Plea for Consistency C.R. S," vol. 16, pp. 267–275, 2007.
- [75] Tao Y, Bai J, Pachauri RK, Sharma A. Parameter extraction of photovoltaic modules using a heuristic iterative algorithm. Energy Convers Manag 2020;224:113386. <https://doi.org/10.1016/j.enconman.2020.113386>.
- [76] Shongwe S, Hanif M. Comparative analysis of different single-diode PV modeling methods. IEEE J Photovoltaics 2015;5(3):938–46.
- [77] Piliouguine M, Guejia-Burbano RA, Petrone G, Sánchez-Pacheco FJ, Mora-López L, Sidrach-de-Cardona M. Parameters extraction of single diode model for degraded photovoltaic modules. Renew Energy 2021;164:674–86. <https://doi.org/10.1016/j.renene.2020.09.035>.